

## An Experimental Study on Flow Boiling Critical Heat Flux on Axisymmetric Sudden Expansion Channel

Yong Jin Kim<sup>a</sup>, Sub Lee Song<sup>a</sup>, Sang Ki Moon<sup>b</sup>, Soon Heung Chang<sup>a</sup>, Yong Hoon Jeong<sup>a\*</sup>

<sup>a</sup>Department of Nuclear and Quantum Engineering, Korea Advanced Institute of Science and Technology, 291 Daehak-ro, Yuseong-gu, Daejeon 34141, Republic of Korea

<sup>b</sup>Korea Atomic Energy Research Institute, 111, Daedeok-daero 989beon-gil, Yuseong-gu, Daejeon, 34057, Korea

\*Corresponding author: jeongyh@kaist.ac.kr

### 1. Introduction

Cladding of the nuclear fuel can be deformed when it experiences rapid temperature and pressure change in severe accident condition. Cladding deformation can change coolant flow path so cooling of core can be affected. In order to mitigate further accident progress, core should be cooled even after accident. Thus, precise knowledge of heat transfer characteristics in deformed cladding should be gathered to enhance safety of nuclear power plant in accident condition. There are many previous studies related to heat transfer characteristics[1] in except for critical heat flux(CHF). In this experiment, CHF was experimentally measured on test section with sudden expansion flow path.

### 2. Experimental Apparatus

#### 2.1 Experimental Loop and Procedure

Experiment was conducted at KAIST flow boiling experimental loop. Fig. 1 shows schematic diagram of loop which consisted of a pump, an electromagnetic flow meter, an electric pre-heater, a condenser and a surge tank. DI water under atmospheric condition was used as working fluid. Electricity for test section heating was supplied by 75kW DC power rectifier, which has specification of 25VX3000A. Data of mass flow, temperature and pressure were gathered by data acquisition system Agilent 34972A.

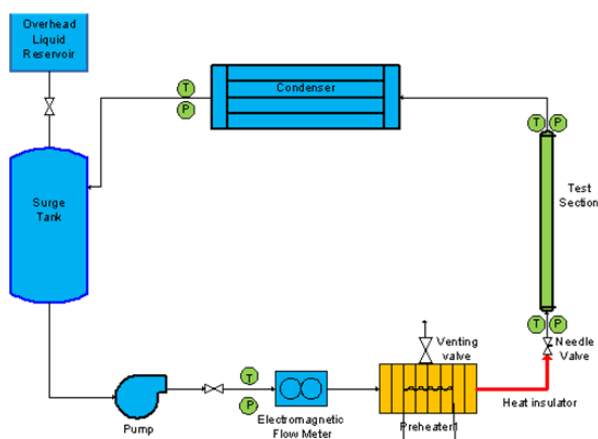


Fig. 1. Schematic diagram of KAIST flow test loop

Prior to the experiment, preheating of the DI water was preceded to remove non-condensing gases. Preheating process took an hour and then subcooling temperature and mass flux were adjusted for each experiment cases. During the experiment, heat flux applied to test section was increased about 20kW/m<sup>2</sup> after thermal equilibrium was achieved. It continued until CHF occurs in test section, which was detected by sudden temperature rise or sudden glowing of test section.

Test matrix for CHF experiments is shown in Table I. Experimental loop was under atmospheric pressure and DI water was flowed upward vertically. Four mass flux cases from 50 to 200kg/m<sup>2</sup>s and two inlet subcooling cases were chosen for experiment condition.

Table I. Test matrix

Pressure(kPa)	101.3
Inlet Mass Flux(kg/m <sup>2</sup> s)	50, 100, 150, 200
Inlet Subcooling(°C)	50, 25
Working Fluid	DI Water

#### 2.2 Design of Test Section

In this experiment, test section with sudden expansion was designed to simulate partial blockage of flow path. The flow path suddenly contracted from the original diameter, and then it suddenly expanded into the original diameter. Sudden contraction and expansion instead of gradual diameter change to simplify flow field near diameter changing part. SUS304 tubes were connected by low temperature welding method to prevent change properties of tube at welded part.

Since the test section is heated directly by joule heating, heat flux through wall is dependent on diameter and thickness of test section. In this experiment, diameter of test section changes so thickness of test section should be adjusted to apply uniform heat flux. Following equation shows relation between heat flux and test section geometry. Here,  $\rho$  is specific resistance,  $t$  is wall thickness and  $D$  is diameter of tube.

$$q'' = \frac{I^2 R}{\pi DL} = \frac{\rho I^2}{\pi^2} \cdot \frac{1}{Dt^2 + D^2 t} \quad (1)$$

Geometry of test section and location of thermocouples are shown in Fig. 2. Surface temperature of test section was measured by K-type thermocouples which are installed along the test section. The tip of each thermocouple was contacted on the test section surface by ceramic jig around the test section.

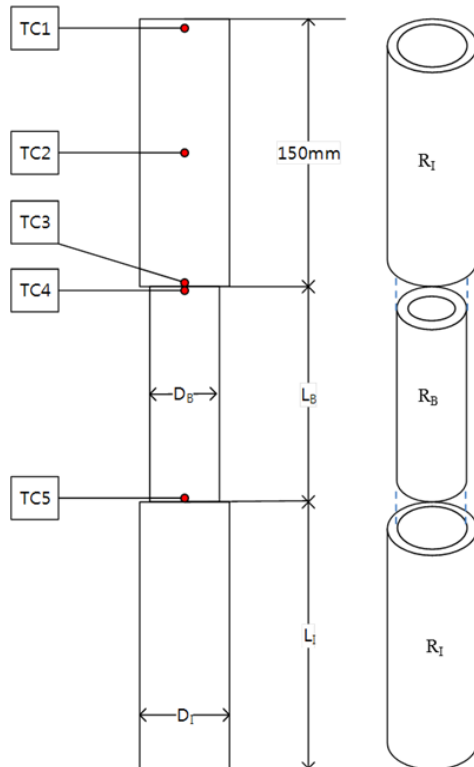


Fig. 2. Test section and location of thermocouples

Specific geometry information, especially about channel diameter of test section is shown in Table II. The blockage ratio \$\epsilon\$ was defined as ratio the ratio between diameter of blocked part and inlet part. Three different blocked diameter of was used. Those are 4 mm, 6 mm, and 8 mm, and the blockage ratio was 2.5, 1.67, and 1.25, respectively. Total heated length was fixed as 400mm and blockage length \$L\_B\$ was 100mm.

Table II. Geometry of test section

\$D_I\$	\$D_B\$	\$\epsilon\$	\$t\$
10mm	8mm	1.25	1.45mm
	6mm	1.67	2.23mm
	4mm	2.5	3.61mm

### 3. Results and Discussion

In this experiment, CHF occurred at two locations, which are test section outlet(TC1) and sudden expansion point(TC3). Experiment results are shown in Fig. 3. CHF occurred at test section outlet when expansion ratio was low(\$\epsilon < 1.5\$) or mass flux was low(\$50\text{kg/m}^2\text{s}\$). On the other hand, premature CHF occurred at sudden expansion point when expansion ratio was high(\$\epsilon > 1.5\$) and mass flux was high.

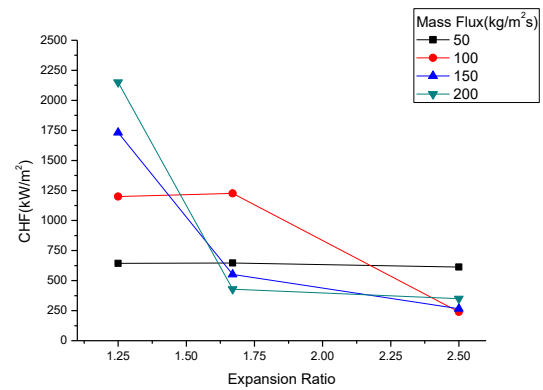


Fig. 3. Experimental results for 50K subcooling

#### 3.1. CHF at test section outlet

When either expansion ratio was lower than 1.5 or mass flux was \$50\text{kg/m}^2\text{s}\$, CHF occurred at test section outlet. Results were compared with the Macbeth's CHF correlation[2]. It is suitable to apply to result of this experiment because of its applicable range. It showed good agreement as shown in Fig. 4.

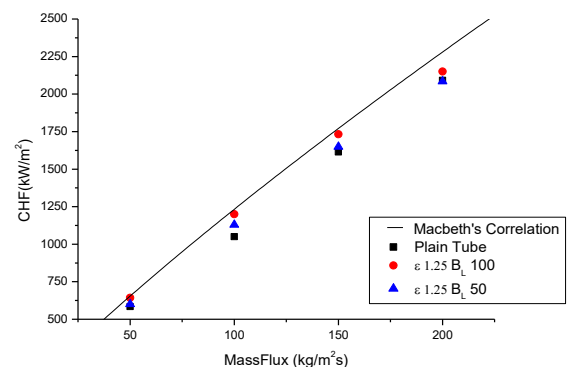


Fig. 4. CHF at test section outlet with reference experiment and Macbeth's correlation

#### 3.2 CHF at Sudden Expansion Point

When both expansion ratio was larger than 1.5 and mass flux was high, CHF was occurred at sudden expansion point. When CHF occurred at sudden

expansion point, the value of CHF was much smaller than expected CHF of plain test section with same experimental condition. It was about 200~500kW/m<sup>2</sup> which was calculated to be nearly saturated condition of working fluid at sudden expansion point. It seems that premature CHF at this point was affected by bubble generation at OSV point so nucleated bubble in sudden expansion flow channel was investigated.

In order to understand motion of bubble in recirculation zone, flow characteristic[3,4] and force acting on bubble[5] was investigated. At sudden expansion point, recirculation flow is induced by flow separation. Backflow velocity in recirculation flow varies at different axial location, which has largest value near midpoint of recirculation.

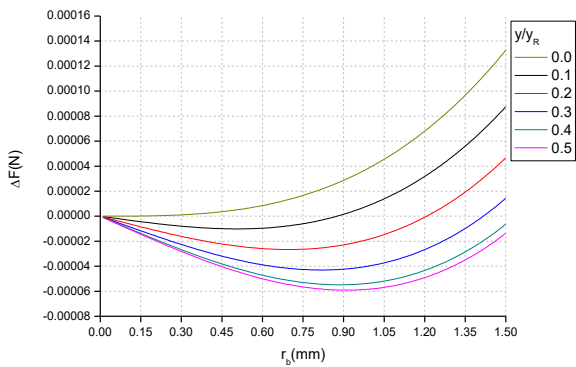
Free bubble detached from wall experiences various force such as buoyancy force, drag force and lift force. Among these forces, buoyancy force  $F_B$  and drag force  $F_D$  are the major forces that exert vertically.

$$F_B = (\rho_f - \rho_g)Vg = \frac{4\pi}{3}(\rho_f - \rho_g)gr_b^3 \quad (2)$$

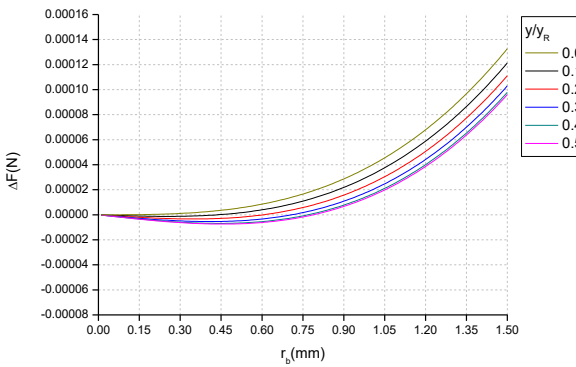
$$F_D = \frac{1}{2}C_D\pi\rho_f r_b^2 \|u\|u \quad (3)$$

$\rho_f, \rho_g$  are saturation density of fluid,  $r_b$  is bubble radius,  $u$  is relative velocity between bubble center and surrounding fluid.  $C_D$  is drag coefficient which can be obtained by  $C_D=48/Re$ . From expressions of force above, drag force is affected by both bubble size and velocity of fluid while buoyancy force is affected by bubble size only. It means that direction of buoyancy force is always upward while direction of drag force changes by surrounding flow.

Fig. 5 and Fig. 6 shows buoyancy force and drag force difference calculated from bubble radius and streamwise velocity in recirculation zone. In both figure, expansion ratio  $\epsilon$  is 2.5 and (a) for 200kg/m<sup>2</sup> s, (b) for 50 kg/m<sup>2</sup> s for mass flux condition.  $y$  is axial distance from sudden expansion point and  $y_R$  is the reattachment point of sudden expansion flow. Velocity profile for calculation was assumed based on previous experimental studies include Abe et al[4]. Maximum backflow velocity was about 0.2 times of velocity at channel center and it was found near midpoint of recirculation zone. Backflow velocity profile was quite symmetric distribution along the recirculation zone, thus in this calculation, it was assumed as sinusoidal form. In  $y$ -axis, the force difference  $\Delta F$  is shown which has positive value when buoyancy force is larger. In Fig. 5,

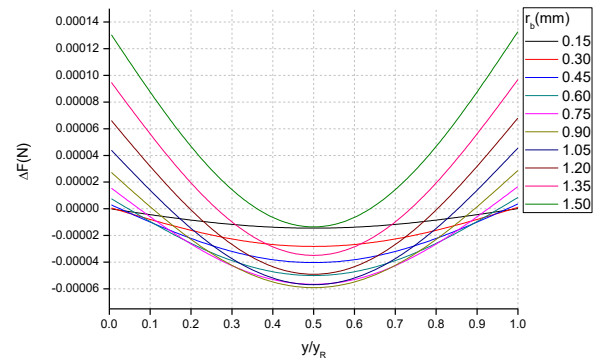


(a)  $G = 200 \text{ kg/m}^2 \text{ s}$

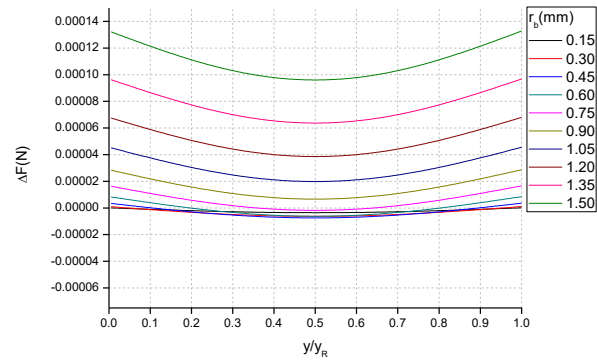


(b)  $G = 50 \text{ kg/m}^2 \text{ s}$

Fig. 5. Force difference by bubble diameter



(a)  $G = 200 \text{ kg/m}^2 \text{ s}$



(b)  $G = 50 \text{ kg/m}^2 \text{ s}$

Fig. 6. Force difference by axial location

as mass flux is higher, which means backflow velocity near wall is also higher, drag force on more bubble is larger than buoyancy force so more bubbles can be stagnant or flow downward. Buoyancy force is proportional to cube of bubble radius while drag force is proportional to bubble radius because drag coefficient  $C_D$  is inversely proportional to radius of bubble. Also, surrounding fluid velocity affects only on the drag force so bubbles that have same diameter will experience same buoyancy force while drag force will be different from its surrounding fluid velocity.

In Fig. 6,  $\Delta F$  at different axial location  $y$  is shown. As mentioned before, velocity profile was assumed as sinusoidal form, so force profile shape is symmetrical. Drag force on bubble increase when streamwise velocity increases. As mass flux increases, more bubbles will be under larger downward drag force, which will lead to downward bubble motion or stagnant in recirculation zone. At the same time, bubbles under smaller drag force at lower axial location will rise due to buoyancy force. Then, bubbles will be accumulated near midpoint of recirculation zone and it would increase local void fraction which can cause premature CHF. It is shown in Fig. 7.

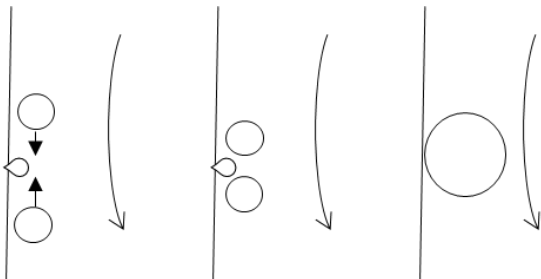


Fig. 7. Local bubble accumulation in recirculation flow

For more precise and quantified analysis of bubble motion under recirculation flow, visualization experiment and computational analysis is in progress.

#### 4. Conclusion

Critical heat flux on sudden expansion flow path was experimentally investigated. Experimental cases with low expansion ratio ( $\epsilon < 1.5$ ) or low mass flux, CHF occurred at test section outlet. CHF was slightly enhanced compared with plain tube experiment. By this research, it was found that for high expansion ratio, CHF can be occurred at sudden expansion point. Experimental cases with both high expansion ratio ( $\epsilon > 1.5$ ) and high mass flux, premature CHF occurred at the sudden expansion point. Force difference between buoyancy force and drag force which are affected by bubble radius and streamwise velocity near wall was analyzed with assumptions. It was induced by local void fraction increase caused by bubble stagnation from force difference on bubbles. Flow characteristics and

bubble dynamics in sudden expansion flow should be further investigated to reduce assumptions applied on analysis.

#### ACKNOWLEDGEMENTS

This research was supported by the KUSTAR-KAIST Institute, KAIST, Korea.

#### REFERENCES

- [1] C. Grandjean, A state of the art review of past programs devoted to fuel behaviour under LOCA conditions—part 2: impact of clad swelling upon assembly cooling, IRSN/DPAM/SEMCA 2006-183.
- [2] R.V. Macbeth, BURN-OUT ANALYSIS. PART 3. THE LOW-VELOCITY BURN-OUT REGIME, No. AEEW-R-222. United Kingdom At. Energy Authority. React. Group. At. Energy Establ. Winfrith, Dorset, Engl. (United Kingdom). (1963).
- [3] J.K. Eaton, J.P. Johnston, A Review of Research on Subsonic Turbulent Flow Reattachment, AIAA J. 19 (1981) 1093–1100. doi:10.2514/3.60048.
- [4] K. Abe, T. Kondoh, Y. Nagano, A new turbulence model for predicting fluid flow and heat transfer in separating and reattaching flows—I. Flow field calculations, Int. J. Heat Mass Transf. 37 (1994) 139–151.
- [5] J. Magnaudet, I. Eames, The Motion of High-Reynolds-Number Bubbles in Inhomogeneous Flows, Annu. Rev. Fluid Mech. 32 (2000) 659–708.